iScience

CellPress
OPEN ACCESS

Article

Long-Term MALT1 Inhibition in Adult Mice Without Severe Systemic Autoimmunity

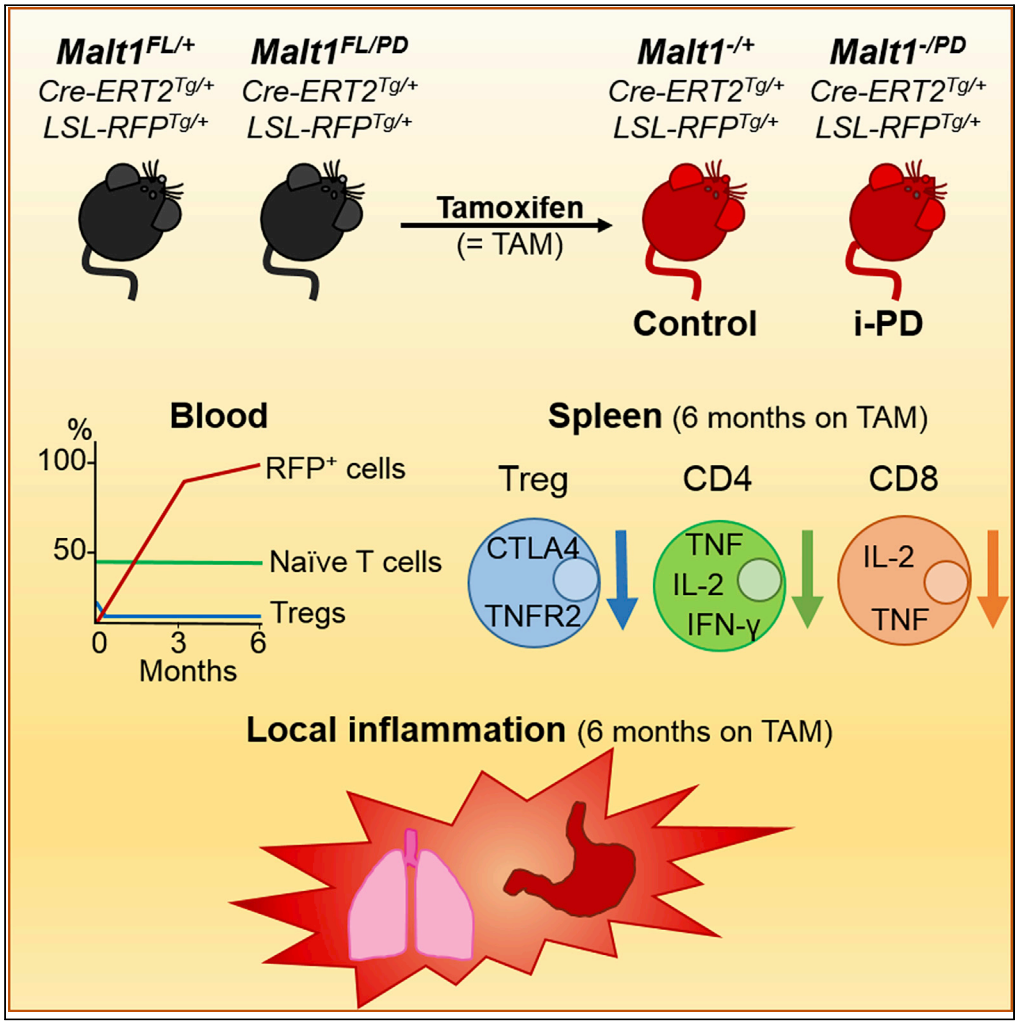

Annelies Demeyer, Yasmine Driege, Ioannis Skordos, ..., Dirk Elewaut, Jens Staal, Rudi Beyaert

rudi.beyaert@irc.vib-ugent.be

HIGHLIGHTS

Inducible MALT1 inactivation for up to 6 months in the absence of severe toxicity

MALT1 inactivation in adult mice decreases Tregs without effector T cell activation

Long-term MALT1 inactivation results in tertiary lymphoid structure formation

MALT1 inhibition in prenatal or adult life has a different outcome

Demeyer et al., iScience *23*, 101557
October 23, 2020
https://doi.org/10.1016/j.isci.2020.101557

iScience

CellPress
OPEN ACCESS

Article

Long-Term MALT1 Inhibition in Adult Mice Without Severe Systemic Autoimmunity

Annelies Demeyer,[1,2] Yasmine Driege,[1,2] Ioannis Skordos,[1,2] Julie Coudenys,[1,3] Kelly Lemeire,[1,2] Dirk Elewaut,[1,3] Jens Staal,[1,2,4] and Rudi Beyaert[1,2,4,5,*]

SUMMARY

The protease MALT1 is a key regulator of NF-κB signaling and a novel therapeutic target in autoimmunity and cancer. Initial enthusiasm supported by preclinical results with MALT1 inhibitors was tempered by studies showing that germline MALT1 protease inactivation in mice results in reduced regulatory T cells and lethal multi-organ inflammation due to expansion of IFN-γ-producing T cells. However, we show that long-term MALT1 inactivation, starting in adulthood, is not associated with severe systemic inflammation, despite reduced regulatory T cells. In contrast, IL-2-, TNF-, and IFN-γ-producing CD4$^+$ T cells were strongly reduced. Limited formation of tertiary lymphoid structures was detectable in lungs and stomach, which did not affect overall health. Our data illustrate that MALT1 inhibition in prenatal or adult life has a different outcome and that long-term MALT1 inhibition in adulthood is not associated with severe side effects.

INTRODUCTION

The paracaspase MALT1 is an important player in innate and adaptive immune signaling (Ruland and Hartjes, 2019). MALT1 is best known for its role in T cell receptor (TCR) signaling leading to nuclear factor (NF)-κB-dependent gene expression, which mediates the activation and proliferation of conventional T cells as well as the development of regulatory T cells (Tregs). Upon TCR triggering, MALT1 is activated as part of the so-called CARD11/BCL10/MALT1 (CBM) complex, where MALT1 functions as a scaffolding protein to recruit the E3 ubiquitin ligase TRAF6 and activate the IκB kinase complex, leading to NF-κB activation (Sun et al., 2004; Oeckinghaus et al., 2007; Lork et al., 2019). TCR engagement also activates MALT1 proteolytic activity, leading to the cleavage of specific substrates (Ruland and Hartjes, 2019). Some of these MALT1 substrates, such as the deubiquitinases A20 and CYLD (Staal et al., 2011; Coornaert et al., 2008), and the mRNA-destabilizing proteins Regnase-1, Roquin-1, and Roquin-2 (Jeltsch et al., 2014; Uehata et al., 2013) are well-known critical negative regulators of pro-inflammatory gene expression whose cleavage is believed to further fine-tune TCR-induced gene expression. Importantly, inhibition of MALT1 enzymatic activity does not influence its scaffolding function, and downstream IκB kinase activation is therefore not affected (Bardet et al., 2018). In fact, specific inhibition of MALT1 enzymatic activity revealed a unique transcriptional fingerprint of MALT1 protease activity, indicating that the proteolytic activity of MALT1 can regulate signaling pathways well beyond NF-κB (Bardet et al., 2018).

MALT1 proteolytic activity is essential to drive T cell survival and expansion (Bardet et al., 2018). Similarly, MALT1 proteolytic activity is essential for the survival and proliferation of certain cancer cells, including ABC-type diffuse large B cell lymphoma and mantle cell lymphoma (Juilland and Thome, 2016). Moreover, MALT1 inhibition may also indirectly decrease tumor growth by interfering with the immune-suppressive function of Tregs (Di Pilato et al., 2019; Rosenbaum et al., 2019). Therefore, the therapeutic potential of MALT1 inhibition in autoimmune disease and cancer has raised a lot of interest and led to the development of potent small compound MALT1 inhibitors (Bardet et al., 2018). Several preclinical studies already showed a protective effect of pharmacological MALT1 inhibition in murine models of multiple sclerosis (Mc Guire et al., 2014), arthritis (Martin et al., 2020b), lymphoma (Fontan et al., 2012; Nagel et al., 2012; Dai et al., 2017; Jacobs et al., 2020), and glioblastoma (Jacobs et al., 2020). Noteworthy, a first-in-human phase I clinical study in participants with relapsed/refractory B-cell non-Hodgkin lymphoma and chronic lymphocytic leukemia has recently been initiated (https://clinicaltrials.gov/ct2/show/NCT03900598). A

[1]Center for Inflammation Research, VIB, Technologiepark-Zwijnaarde 71, 9052 Ghent, Belgium

[2]Department of Biomedical Molecular Biology, Ghent University, Technologiepark-Zwijnaarde 71, 9052 Ghent, Belgium

[3]Department of Internal Medicine and Pediatrics, Ghent University, Technologiepark-Zwijnaarde 71, 9052 Ghent, Belgium

[4]Senior author

[5]Lead Contact

*Correspondence: rudi.beyaert@irc.vib-ugent.be

https://doi.org/10.1016/j.isci.2020.101557

major concern was, however, raised by several independent studies showing that knock-in mice constitutively expressing a catalytically inactive MALT1 "protease-dead" mutant (*Malt1*-PD mice) rapidly develop lethal autoimmune inflammation in multiple organs (Gewies et al., 2014; Jaworski et al., 2014; Yu et al., 2015; Bornancin et al., 2015; Demeyer et al., 2019; Martin et al., 2019). This was somewhat surprising because a previous study had shown that pharmacological inhibition of MALT1 in mice for up to 3 weeks does not cause any side effects (Mc Guire et al., 2014). One major difference, however, between the genetic models and inhibitor treatment is that germline *Malt1*-PD mice lack protease activity at conception or at a very young age, whereas MALT1 inhibitor treatment is done in adult life. In this context, the severe reduction in thymic Tregs in *Malt1*-PD mice, which are mostly formed at young age (Fontenot et al., 2005), has been suggested to be at the origin of the severe autoimmune phenotype of these mice (Jaworski et al., 2014; Gewies et al., 2014; Demeyer et al., 2019; Baens et al., 2018). However, recent studies showed that MALT1 protease activity is also critical for maintaining Treg function (Cheng et al., 2019; Rosenbaum et al., 2019), implicating a risk for autoimmunity when MALT1 protease activity is only lost in adulthood. To have a clear view on the safety of long-term inhibition of MALT1 in adults, we have therefore generated a full-body tamoxifen-inducible *Malt1*-i-PD mouse model, which allowed us to monitor the effect of MALT1 inactivation in adult mice for up to 6 months.

RESULTS AND DISCUSSION

Long-Term Inducible MALT1 Inactivation in Adult Mice Decreases Tregs Without Increasing Effector T Cell Activation

To obtain a full-body tamoxifen-inducible *Malt1*-i-PD mouse model, we first generated $Malt1^{PD/FL}$ or $Malt1^{+/FL}$ mice with a tamoxifen-inducible Cre-ERT2 in one *Rosa26* allele (Hameyer et al., 2007) and a LoxP-stop-LoxP (LSL)-RFP reporter for Cre activity in the other *Rosa26* allele (Luche et al., 2007) (Figure 1A). Upon tamoxifen administration, the floxed third exon of the $Malt1^{FL}$ allele and the floxed stop cassette of the RFP reporter are removed by Cre-mediated recombination. In this way we obtained $Malt1^{+/-}$ (= control) and $Malt1^{PD/-}$ (= *Malt1*-i-PD) mice with RFP^+ cells representing cells in which Cre-ERT2 was active. Mice received tamoxifen for 5 days via oral gavage and were then kept on tamoxifen containing feed to prevent repopulation by $Malt1^{+/FL}$ or $Malt1^{PD/FL}$ bone marrow-derived cells. To monitor the efficiency of Cre recombination, RFP expression was assessed in blood cells at several time points following the start of tamoxifen treatment. After 2–3 months the majority of mice had 70% to 85% RFP^+ blood cells (Figure 1B). *Malt1*-i-PD mice were sacrificed after 6 months tamoxifen treatment, and most mice had up to 90% or more $CD3^+$ RFP^+ cells in their spleen at this endpoint (Figure 1C). Mice showing less than 70% RFP^+ cells were excluded from the analysis in subsequent experiments. MALT1 protease deficiency in *Malt1*-i-PD mice could be confirmed by the lack of CYLD, BCL10, and HOIL-1 cleavage in phorbol 12-myristate 13-acetate (PMA)/ionomycin-stimulated splenocytes (Figure 1D).

Germline inactivation of MALT1 protease activity in *Malt1*-PD mice is associated with a severe reduction of Tregs and activation of $CD4^+$ and $CD8^+$ T cells, leading to multi-organ inflammation (Jaworski et al., 2014; Gewies et al., 2014; Bornancin et al., 2015; Demeyer et al., 2019). In our study, *Malt1*-i-PD circulating Treg levels were already decreased upon 1 week tamoxifen treatment and reached about 30% of the levels present in control mice after 6 months (Figure 1E). However, despite this significant drop in Tregs, blood $CD4^+$ and $CD8^+$ T cell activation remained unaltered between control and *Malt1*-i-PD mice (Figures 1F and 1G). At endpoint, *Malt1*-i-PD and control mice had similar amounts of thymic and splenic $CD4^+$ and $CD8^+$ T cells (Figures 2A and 2C). However, the amount of thymic Tregs and splenic Tregs had dropped to 25% and 30%, respectively, compared with control mice (Figures 2B and 2D). Also, Treg expression of the functionality markers CTLA4 and TNFR2 was severely reduced upon MALT1 inactivation (Figure 2E), which is in agreement with the described role of MALT1 protease activity in TCR-induced CTLA4 expression in Tregs (Rosenbaum et al., 2019). Importantly, the significant drop in CTLA4- and TNFR2-expressing splenic Tregs in *Malt1*-i-PD mice did not result in overt splenic $CD4^+$ and $CD8^+$ T cell activation (Figure 2F). Moreover, the number of TNF-, IL-2-, and IFN-γ-producing $CD4^+$ T cells was strongly reduced upon long-term MALT1 inactivation (Figure 2G). Similar results were obtained for $CD8^+$ T cells, with the surprising exception for IFN-γ-producing $CD8^+$ T cells, which were not altered (Figure 2H). Importantly, the reduction in IFN-γ-producing $CD4^+$ T cells upon long-term inducible MALT1 inactivation is in strong contrast to the increase in IFN-γ-producing $CD4^+$ T cells described in constitutive germline *Malt1*-PD mice (Jaworski et al., 2014; Demeyer et al., 2019; Martin et al., 2019). Total B cell levels were similar at endpoint (Figure 3A), but the frequency of MZ B cells was reduced in *Malt1*-i-PD mice (Figure 3B), which is similar to the previously described drop in *Malt1*-PD mice (Demeyer et al., 2019; Gewies et al., 2014; Bornancin et al., 2015; Yu et al.,

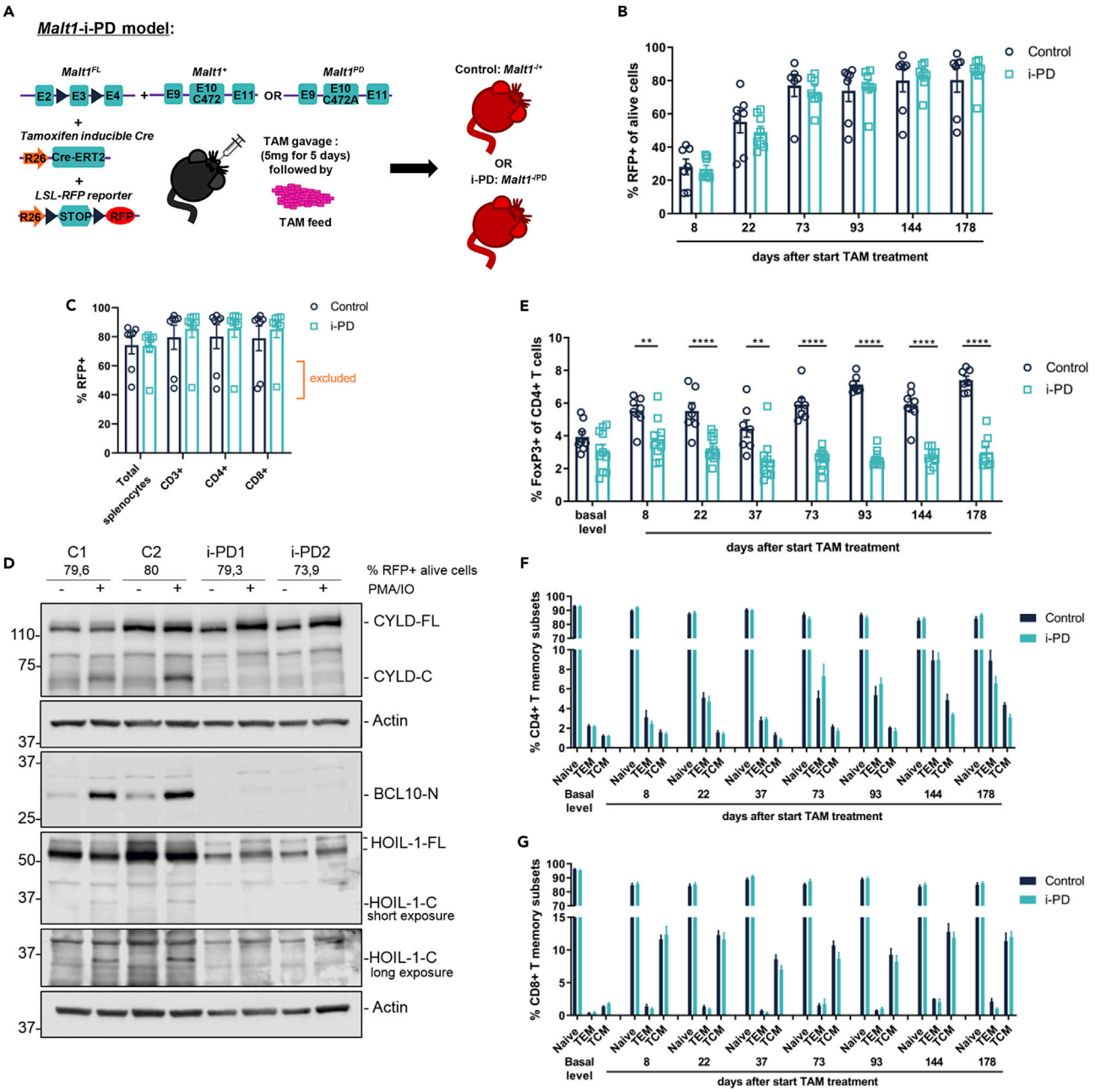

Figure 1. Long-Term Inducible MALT1 Protease Inactivation Reduces Circulating Treg Levels without Changing the Activation Status of CD4$^+$ and CD8$^+$ T Cells

(A) Strategy to generate *Malt1*-i-PD mice.

(B) Frequency of RFP$^+$ alive cells in blood of *Malt1*-i-PD and control mice at several time points after starting tamoxifen treatment.

(C) Frequency of living RFP$^+$ splenocytes, CD3$^+$, CD4$^+$, and CD8$^+$ splenic T cells in *Malt1*-i-PD and control mice after 6 months tamoxifen treatment. Excluded = 3 mice with less than 70% RFP$^+$ alive splenocytes that were excluded for subsequent analysis.

(D) Immunoblot for CYLD, HOIL-1, and cleaved BCL10 on splenocyte extracts of control (C1 and C2) and two different *Malt1*-i-PD mice (i-PD1 and i-PD2) stimulated *in vitro* with PMA and ionomycin (PMA/IO) for 1.5 h to activate MALT1. Frequency of RFP$^+$ splenocytes of these mice is indicated.

(E–G) (E) Frequency of Tregs; (F) naive, effector memory (TEM) and central memory (TCM) CD4$^+$ T cells; and (G) CD8$^+$ T cells in blood before and at several time points after starting tamoxifen treatment.

(B, C, and E–G) Data (control: n = 7 and *Malt1*-i-PD: n = 8) obtained by flow cytometry, presented as mean ± SEM and statistical significance: unpaired two-tailed Student's t test (**p < 0.01; ****p < 0.0001). All data are representative for two independent experiments.

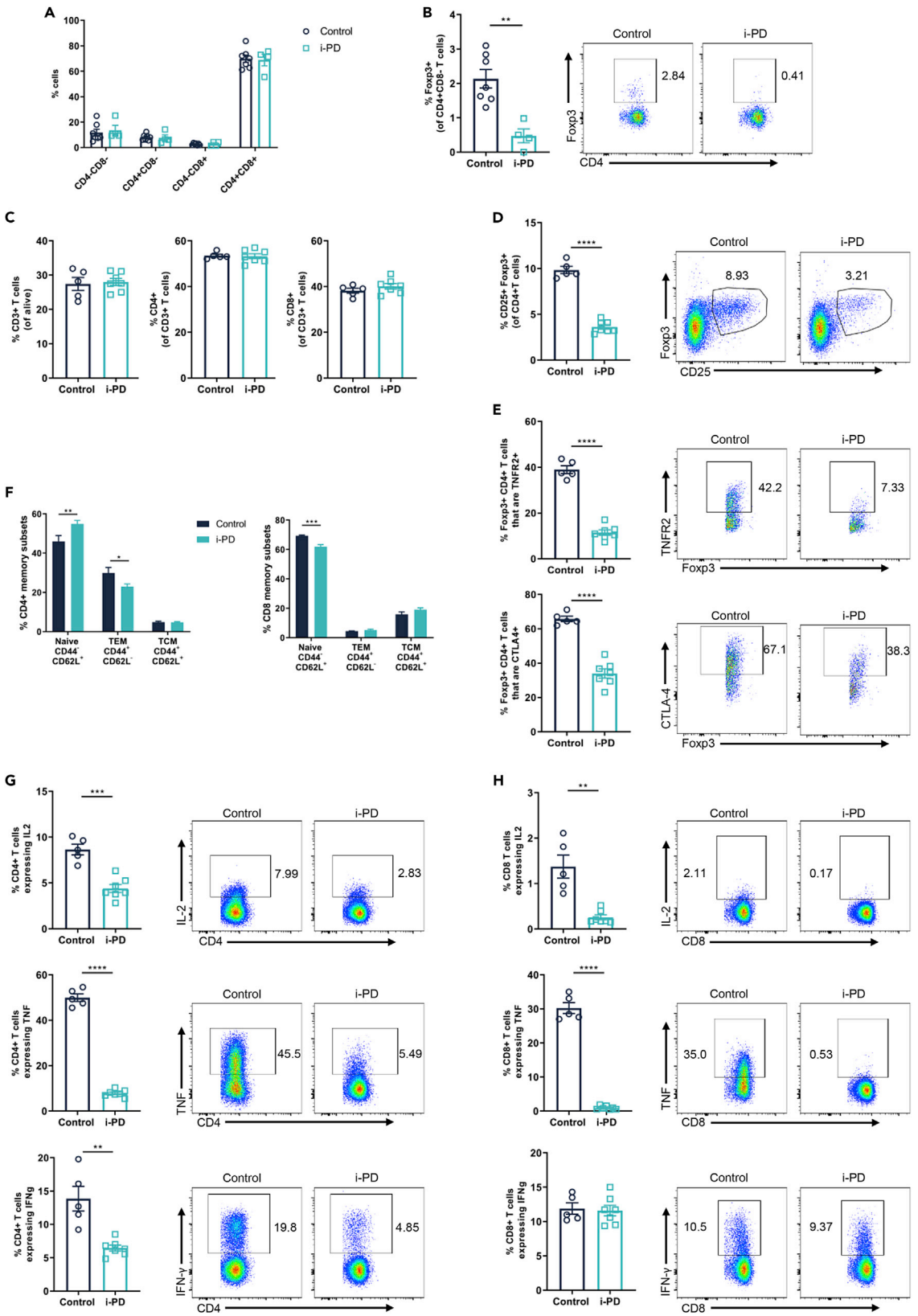
A
% cells
Control
i-PD
CD4-CD8-
CD4+CD8-
CD4-CD8+
CD4+CD8+
B
% Foxp3+ (of CD4+CD8- T cells)
Control
i-PD
2.84
0.41
Foxp3
CD4
C
% CD3+ T cells (of alive)
% CD4+ (of CD3+ T cells)
% CD8+ (of CD3+ T cells)
D
% CD25+ Foxp3+ (of CD4+T cells)
8.93
3.21
CD25
E
% Foxp3+ CD4+ T cells that are TNFR2+
42.2
7.33
TNFR2
% Foxp3+ CD4+ T cells that are CTLA4+
67.1
38.3
CTLA-4
F
% CD4+ memory subsets
% CD8 memory subsets
Naive CD44- CD62L+
TEM CD44+ CD62L-
TCM CD44+ CD62L+
G
% CD4+ T cells expressing IL2
7.99
2.83
IL-2
% CD4+ T cells expressing TNF
45.5
5.49
TNF
% CD4+ T cells expressing IFNg
19.8
4.85
IFN-γ
H
% CD8 T cells expressing IL2
2.11
0.17
% CD8+ T cells expressing TNF
35.0
0.53
% CD8+ T cells expressing IFNg
10.5
9.37

Figure 2. Long-Term Inducible MALT1 Protease Inactivation Reduces Thymic and Splenic Treg Levels Without Changing the Activation Status of Splenic CD4$^+$ and CD8$^+$ T Cells

Malt1-i-PD (n = 4) and control (n = 7) mice were treated with tamoxifen for 6 months, and thymocytes were analyzed at endpoint by flow cytometry.
(A and B) Frequency of (A) CD4$^-$CD8$^-$, CD4$^+$CD8$^-$, CD4$^-$CD8$^+$, and CD4$^+$CD8$^+$ cells and (B) Tregs (Foxp3$^+$CD4$^+$CD8$^-$ T cells).
Malt1-i-PD (n = 6) and control (n = 5) mice were treated with tamoxifen for 6 months, and splenocytes were analyzed at endpoint by flow cytometry.
(C–H) (C) Frequency of CD3$^+$, CD4$^+$, and CD8$^+$ T cells; (D) Tregs (CD25$^+$Foxp3$^+$CD4$^+$ T cells); (E) Tregs expressing TNFR2 or CTLA4; (F) naive, TEM, TCM CD4$^+$, and CD8$^+$ T cells; (G) CD4$^+$ T cells expressing IL-2, TNF, or IFN-γ; and (H) CD8$^+$ T cells expressing IL-2, TNF, or IFN-γ.
Data presented as mean ± SEM and statistical significance: unpaired two-tailed Student's t test (*p < 0.05; **p < 0.01; ***p < 0.001; ****p < 0.0001).
Representative flow cytometry plots showing gating strategy and individual cell frequencies are included. All data are representative for two independent experiments.

2015; Jaworski et al., 2014; Baens et al., 2018). There were no significant differences in the amount of monocytes and different DC populations between control and *Malt1*-i-PD mice (Figure 3C). Together, these results clearly show that long-term inducible inactivation of MALT1 protease activity in adult mice mainly affects the lymphocyte compartment of the immune system. Most importantly and in contrast to constitutive MALT1 protease inactivation by germline engineering, long-term MALT1 protease inactivation in adult mice does not lead to the activation of CD4$^+$ and CD8$^+$ T cells in blood or spleen, despite significantly reduced Treg levels.

Long-Term Inducible MALT1 Inactivation in Adult Mice Does Not Cause Systemic Inflammation

In contrast to the severe and rapid body weight loss that was previously observed in constitutive *Malt1*-PD mice (Demeyer et al., 2019; Yu et al., 2015; Jaworski et al., 2014; Gewies et al., 2014; Bornancin et al., 2015), only a mild reduction in body weight was observed in male, but not female, *Malt1*-i-PD mice at endpoint (Figure 4A). Also, *Malt1*-i-PD mice did not develop severe ataxia that was previously observed in constitutive *Malt1*-PD mice. In addition, whereas constitutive *Malt1*-PD mice were reported to have high serum IFN-γ and TNF levels (Gewies et al., 2014; Demeyer et al., 2019), *Malt1*-i-PD mice only showed a very mild increase in TNF serum levels and no significant difference for IFN-γ, IL-5, IL-10, IL-13, IL-17, and KC (Figure 4B). Jaworski et al. reported IgE and IgG1 autoantibodies reactive against stomach antigens in constitutive *Malt1*-PD mice (Jaworski et al., 2014), whereas Martin et al. reported elevated IgE and IgG1 antibodies reactive against bacterial and food antigens (Martin et al., 2019), although these were not essential for the development of autoimmune inflammation in *Malt1*-PD mice. In our study, no autoantibodies against specific nuclear and cytoplasmic antigens could be detected in serum from *Malt1*-i-PD mice (Figure S1). Together, these results clearly show that, in contrast to constitutive MALT1 protease inactivation by germline engineering, long-term inducible inactivation of MALT1 protease activity in adult mice does not cause systemic inflammation, which is consistent with the absence of effector T cell activation.

Long-Term Inducible MALT1 Inactivation in Adult Mice Induces Tertiary Lymphoid Structures in Specific Tissues

Constitutive *Malt1*-PD mice rapidly develop lethal multi-organ inflammation (Jaworski et al., 2014; Gewies et al., 2014; Bornancin et al., 2015; Demeyer et al., 2019; Martin et al., 2019). In contrast, *Malt1*-i-PD mice looked healthy after 6 months MALT1 inactivation. Spleen size was similar in both *Malt*1-i-PD and control mice (Figure 4C), and macroscopic examination of several other organs also did not show any clinical signs of disease. H&E-stained tissue sections did not reveal inflammation in salivary gland, colon, and liver (Figure 4D). However, almost all *Malt1*-i-PD mice suffered from increased immune cell infiltration in the stomach (Figures 4E and 4G) and lungs (Figures 4F and 4H). It should be mentioned that some control mice also displayed minor immune cell infiltration in stomach and even more in lungs, which may reflect their relatively advanced age. Some of the immune cell infiltrates in *Malt1*-i-PD mice resembled tertiary lymphoid structures (Pipi et al., 2018), which was further supported upon staining for B (B220) and T cells (CD3) (Figures 4I and 4J). Especially in lungs, a separate B cell zone, which is characteristic for inducible bronchus-associated lymphoid tissue formation (Woodland and Randall, 2004), could be observed (Figure 4J). It should be mentioned that stomach and lung inflammation has been described in the case of constitutive *Malt1*-PD mice (Jaworski et al., 2014; Gewies et al., 2014; Bornancin et al., 2015; Yu et al., 2015; Demeyer et al., 2019). Moreover, mice with a Treg-specific loss of MALT1 protease function also suffer from lung inflammation (Cheng et al., 2019). Together, these data demonstrate that, in contrast to the lethal multi-organ inflammation observed upon germline MALT1 protease inactivation, long-term inducible inhibition of MALT1 protease activity in adult mice is only associated with local immune cell infiltration in stomach and lungs.

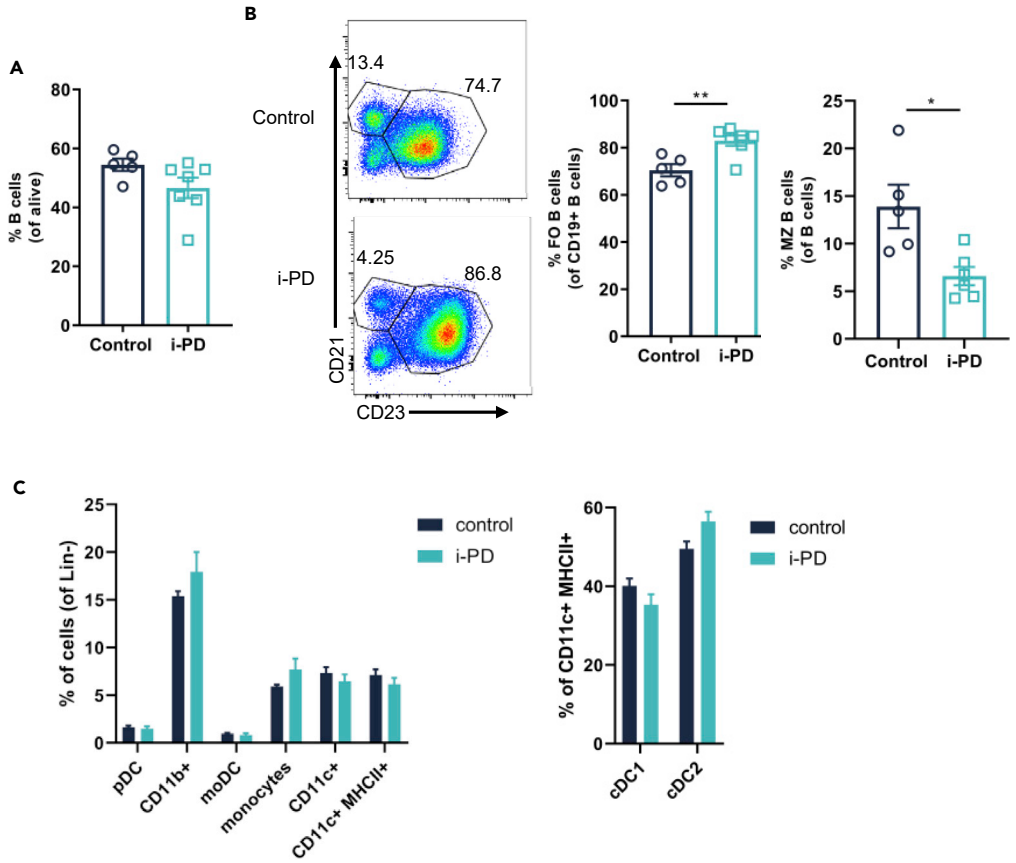

Figure 3. Long-Term Inducible MALT1 Protease Inactivation Reduces MZ B Cell Levels and has No Effect on Monocytes and Different DC Populations

Malt1-i-PD (n = 7) and control (n = 5) mice were treated with tamoxifen for 6 months, and splenocytes were analyzed at endpoint by flow cytometry.

(A–C) Frequency of (A) total B cells, (B) FO B cells and MZ B cells, and (C) monocytes and different DC populations. Data obtained by flow cytometry, presented as mean ± SEM and statistical significance: unpaired two-tailed Student's t test (*$p < 0.05$; **$p < 0.01$). Representative flow cytometry plots showing gating strategy and individual B cell frequencies are included in (B). All data are representative for two independent experiments.

In conclusion, our data indicate that long-term inhibition of MALT1 proteolytic activity in adult life is relatively safe and does not lead to destructive autoimmune inflammation as previously described upon germline inactivation of MALT1. These discrepancies most likely reflect the known key role of MALT1 proteolytic activity in thymic Treg development early during life, whereas peripheral Treg generation has been shown to be less MALT1 dependent (Brustle et al., 2015). In addition, MALT1 protease inhibition results in reduced cytokine production by T cells in the periphery, which might lead to a new equilibrium between residual Tregs on one side and lower cytokine-producing T cells on the other side. There is still a caveat of potential local autoimmunity in lungs and stomach upon MALT1 inhibition, which may reflect a specific role for MALT1 in immune tolerance toward locally displayed antigens. Interestingly, a recent study in rat and dog (Martin et al., 2020b) reported decreased Treg numbers and immune infiltration in specific organs, but no ataxia and lethal autoimmunity upon prolonged treatment with a novel MALT1 inhibitor (MLT-943), which is in line with our data. Nevertheless, despite an excellent selectivity profile of the used MALT1 inhibitor, it cannot be fully excluded that off-target effects of the inhibitor contribute to the observed side effects in the study of Martin et al. Our data with *Malt1*-i-PD mice, which do not suffer from off-target effects and show that prolonged and specific MALT1 targeting is only associated with mild immune cell infiltration in certain organs (stomach and lungs), therefore indicate that studies using different classes of compounds with improved specificity deserve further evaluation. Going forward, the evaluation of side effects of different classes of small compound inhibitors of MALT1 for the treatment of autoimmune inflammation or cancer should therefore especially focus on these tissues that show

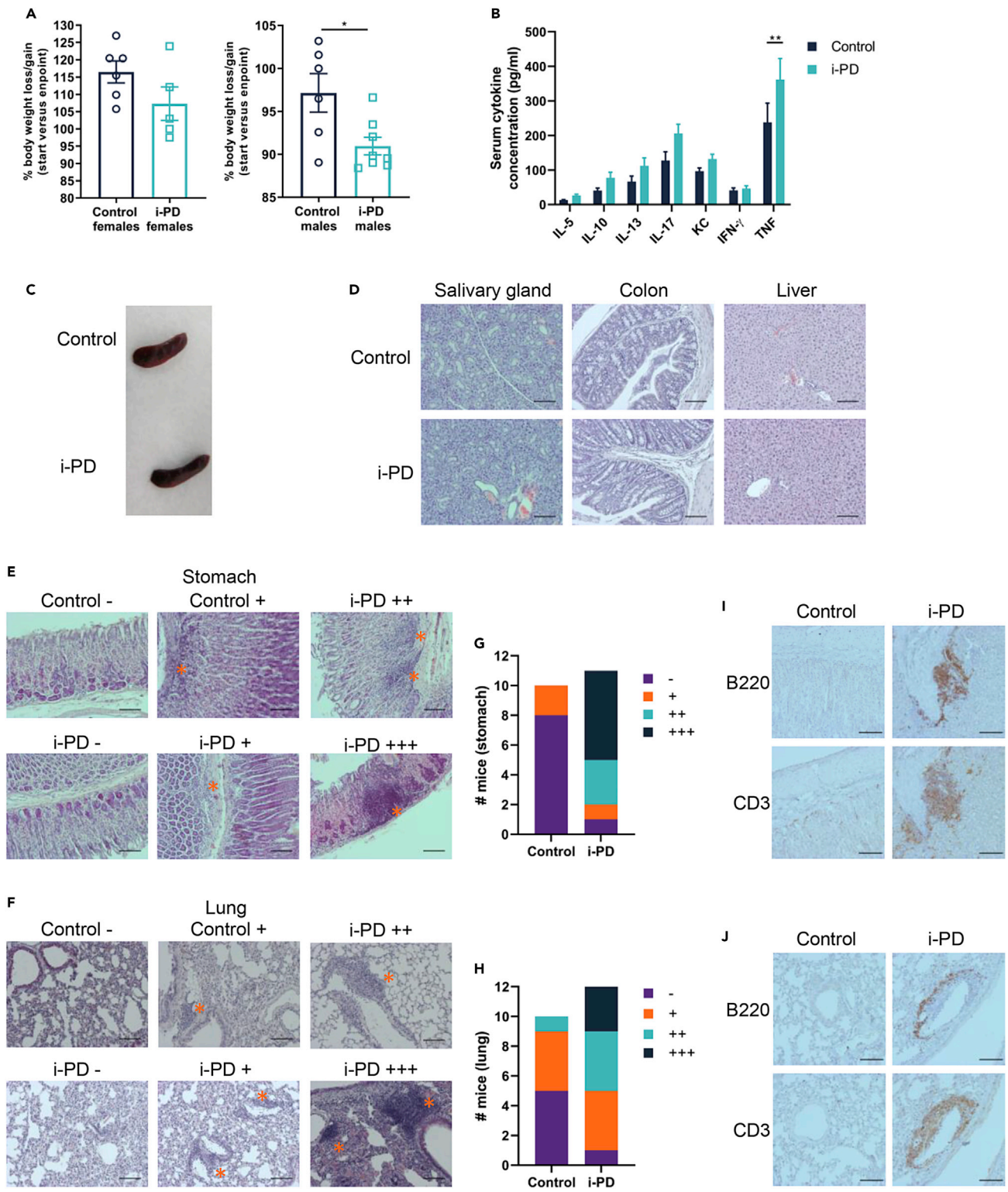

Figure 4. Long-Term Inducible MALT1 Protease Inactivation is Associated with Local Immune Cell Infiltration in Stomach and Lungs

Malt1-i-PD and control mice were treated with tamoxifen for 6 months, and analyzed at endpoint.

(A) Change in body weight of female (control: n = 6 and *Malt1*-i-PD: n = 5) and male (control: n = 6 and *Malt1*-i-PD: n = 8) mice at endpoint compared with their initial weight.

Figure 4. *Continued*

(B) Serum cytokine concentration of *Malt1*-i-PD (n = 12) and control (n = 11) mice.

(C) Representative picture of the spleen of control and *Malt1*-i-PD mice.

(D) Representative picture of H&E staining of salivary gland (control: n = 10 and *Malt1*-i-PD: n = 11), colon (control: n = 6 and *Malt1*-i-PD: n = 6), and liver (control: n = 10 and *Malt1*-i-PD: n = 12).

(E and F) (E) Representative picture of different degrees of immune cell infiltration based on H&E staining of stomach and (F) lung from different control (n = 10) and *Malt1*-i-PD (n = 11) mice. Different degrees of immune cell infiltration (indicated with an asterisk): none (–), minor dispersed infiltration (+), multiple large infiltrations (++), and infiltrations resembling tertiary lymphoid organs (+++).

(G and H) (G) Number of *Malt1*-i-PD and control mice showing the indicated degrees of stomach and (H) lung immune cell infiltration.

(I and J) (I) Representative picture of anti-B220 and anti-CD3 staining of stomach (n = 3) and (J) lung (n = 3) tissue sections from control and *Malt1*-i-PD mice with infiltrations resembling tertiary lymphoid organs (+++).

Scale bars, 100 μm in (D–F) and (I–J); (A and B) mean ± SEM and statistical significance: unpaired 2-tailed Student's t test (*$p < 0.05$; **$p < 0.01$). All data are representative for two independent experiments.

See also Figure S1.

inflammation in our mouse model and in the models used by Martin et al. Similar immune-related adverse effects have been described for immune checkpoint inhibitors targeting CTLA4 (Friedman et al., 2016; Johncilla et al., 2019), which could be related to the observed decrease in CTLA4-expressing Tregs upon inducible MALT1 inhibition. Management strategies developed for those side effects of immune checkpoint inhibition could potentially also be useful to mitigate the risks of MALT1 protease inhibition (Brahmer et al., 2018; Friedman et al., 2016). The here-described inducible mouse model for MALT1 targeting is unique, in the sense that it allows to follow-up mice for a much longer time than possible with small compound MALT1 inhibitors that need daily treatment. Such prolonged studies are essential to increase the successful translation of preclinical mouse studies to patients. While the original enthusiasm of big pharmaceutical companies in therapeutic targeting of MALT1 was strongly tempered by multiple studies reporting a severe autoimmune phenotype of constitutive *Malt1*-PD mice, the results described here can be expected to stir a renewed interest in the development of small compound MALT1 inhibitors for several autoimmune diseases and cancers.

Limitations of the Study

Lack of lethal autoimmunity in our *Malt1*-i-PD mice could still be due to the incomplete inactivation of MALT1. However, partial MALT1 inactivation in our mice mimics pharmacological targeting (Martin et al., 2020a). Conceptually our model is therefore very relevant in the context of therapeutic targeting of MALT1 with small compound inhibitors. Importantly, partial inactivation is what one also observes with most small compounds *in vivo*, exposure of which does not result in a complete and continuous inhibition due to the pharmacokinetic profile of the compound. In addition, there are several partial allosteric inhibitors that only show partial inhibition, known as maximal efficacy. This is very well known in the case of GPCRs (Verespy et al., 2016), but also exists for other enzymes such as proteases (Conn et al., 2009). It should be stressed that 2 to 3 months after the start of tamoxifen treatment, the number of RFP^+ cells in the blood is for most mice between 70% and 85% (Figure 1B). Moreover, several mice included for endpoint analysis after 6 months had up to 90% RFP^+ T cells (Figure 1C). (The level of inhibition in T cells is the most important because disease development in *Malt1*-PD mice was previously shown to be driven by defective MALT1 activity in T cells, Demeyer et al., 2019). Moreover, the above level of MALT1 inactivation clearly reduced the number of IL-2-, TNF-, and IFN-γ-producing $CD4^+$ T cells (Figure 2G), which is known to be dependent on MALT1 proteolytic activity (Bardet et al., 2018). Last but not least, MALT1-dependent CYLD, HOIL-1, and BCL10 cleavage was completely abolished in splenocytes isolated from *Malt1*-i-PD mice with more than 70% RFP^+ cells (Figure 1D). Together, these data illustrate that the obtained level of MALT1 inactivation is sufficient to prevent a MALT1-dependent biological response. In future studies, it will be of interest to determine the *in vivo* impact of this specific inhibition of MATL1 protease activity in Malt1-i-PD mice in an autoimmune disease model.

For our experiments we used specific pathogen-free (SPF) mice that might have a different immune status compared with mice housed in a conventional environment. However, a conventional mouse facility suffers from several unknown environmental factors that differ from laboratory to laboratory, which can seriously affect results and hamper reproducibility. SPF conditions have therefore been the standard in most mouse facilities, including ours, for many years. Moreover, we wanted to compare the results of *Malt1*-i-PD mice with previously reported data with constitutive *Malt1*-PD mice that were kept in an SPF facility. Importantly, although both mouse lines were kept in SPF conditions, we could show that *Malt1*-i-PD mice do not phenocopy the severe lethal autoimmunity in *Malt1*-PD mice.

Resource Availability

Lead Contact

Further information and requests for resources and reagents should be directed to and will be fulfilled by the Lead Contact, Rudi Beyaert (Rudi.Beyaert@irc.vib-ugent.be).

Materials Availability

All mouse lines and reagents generated in this study are available from the Lead Contact with a completed Materials Transfer Agreement.

Data and Code Availability

This study did not generate large-scale datasets. Raw data of this article are available from the lead contact upon request.

METHODS

All methods can be found in the accompanying Transparent Methods supplemental file.

SUPPLEMENTAL INFORMATION

Supplemental Information can be found online at https://doi.org/10.1016/j.isci.2020.101557.

ACKNOWLEDGMENTS

We would like to thank the VIB Flow Core and the VIB Bioimaging Core for training, support, and access to the instrument park. M. Baens is acknowledged for providing anti-BCL10 cleavage-specific antibody. Research in the authors' laboratory is supported by grants from the "Fund for Scientific Research Flanders" (FWO), Belgium; "Belgian Foundation Against Cancer", Belgium; Ghent University "Concerted Research Actions" (GOA), Belgium, and the "VIB Grand Challenges Program" (VIB-GC01-C01), Belgium. A.D. was supported by a predoctoral fellowship from the "Agency for Innovation by Science and Technology" (IWT). J.S. was supported by a postdoctoral fellowship from the FWO.

AUTHOR CONTRIBUTIONS

A.D. and J.S. designed the experiments. J.S. and R.B. supervised the work. A.D. performed all the experiments, with the technical assistance of Y.D, except for Figure S1 (done by J.C. under the supervision of D.E.). I.S. contributed to the experiments shown in Figures 2A and 2B. K.L. provided technical assistance for the experiment shown in Figures 4I and 4J. A.D., J.S., and R.B. contributed to the scientific discussion and wrote the manuscript.

DECLARATION OF INTERESTS

In the past, A.D., J.S., and R.B have been involved in a research collaboration and licensing agreement with AstraZeneca and Galapagos, which has been terminated in the meantime. R.B. is inventor on the patent "Inhibitors of MALT1 proteolytic activity and uses thereof,", WO09065897, applicants: VIB and UGent. The authors declare no other competing interests.

Received: May 18, 2020
Revised: September 2, 2020
Accepted: September 10, 2020
Published: October 23, 2020

REFERENCES

Baens, M., Stirparo, R., Lampi, Y., Verbeke, D., Vandepoel, R., Cools, J., Marynen, P., de Bock, C.E., and Bornschein, S. (2018). Malt1 self-cleavage is critical for regulatory T cell homeostasis and anti-tumor immunity in mice. Eur. J. Immunol. *48*, 1728–1738.

Bardet, M., Unterreiner, A., Malinverni, C., Lafossas, F., Vedrine, C., Boesch, D., Kolb, Y., Kaiser, D., Gluck, A., Schneider, M.A., et al. (2018). The T-cell fingerprint of MALT1 paracaspase revealed by selective inhibition. Immunol. Cell Biol. *96*, 81–99.

Bornancin, F., Renner, F., Touil, R., Sic, H., Kolb, Y., Touil-Allaoui, I., Rush, J.S., Smith, P.A., Bigaud, M., Junker-Walker, U., et al. (2015). Deficiency of MALT1 paracaspase activity results in unbalanced regulatory and effector T and B cell responses leading to multiorgan inflammation. J. Immunol. *194*, 3723–3734.

Brahmer, J.R., Lacchetti, C., Schneider, B.J., Atkins, M.B., Brassil, K.J., Caterino, J.M., Chau, I., Ernstoff, M.S., Gardner, J.M., Ginex, P., et al. (2018). Management of immune-related adverse events in patients treated with immune

checkpoint inhibitor therapy: American society of clinical oncology clinical practice guideline. J. Clin. Oncol. *36*, 1714–1768.

Brustle, A., Brenner, D., Knobbe-Thomsen, C.B., Cox, M., Lang, P.A., Lang, K.S., and Mak, T.W. (2015). MALT1 is an intrinsic regulator of regulatory T cells. Cell Death Differ. *24*, 1214–1223.

Cheng, L., Deng, N., Yang, N., Zhao, X., and Lin, X. (2019). Malt1 protease is critical in maintaining function of regulatory T cells and may Be a therapeutic target for antitumor immunity. J. Immunol. *202*, 3008–3019.

Conn, P.J., Christopoulos, A., and Lindsley, C.W. (2009). Allosteric modulators of GPCRs: a novel approach for the treatment of CNS disorders. Nat. Rev. Drug Discov. *8*, 41–54.

Coornaert, B., Baens, M., Heyninck, K., Bekaert, T., Haegman, M., Staal, J., Sun, L., Chen, Z.J., Marynen, P., and Beyaert, R. (2008). T cell antigen receptor stimulation induces MALT1 paracaspase-mediated cleavage of the NF-kappaB inhibitor A20. Nat. Immunol. *9*, 263–271.

Dai, B., Grau, M., Juilland, M., Klener, P., Horing, E., Molinsky, J., Schimmack, G., Aukema, S.M., Hoster, E., Vogt, N., et al. (2017). B-cell receptor-driven MALT1 activity regulates MYC signaling in mantle cell lymphoma. Blood *129*, 333–346.

Demeyer, A., Skordos, I., Driege, Y., Kreike, M., Hochepied, T., Baens, M., Staal, J., and Beyaert, R. (2019). MALT1 proteolytic activity suppresses autoimmunity in a T cell intrinsic manner. Front Immunol. *10*, 1898.

Di Pilato, M., Kim, E.Y., Cadilha, B.L., Prussmann, J.N., Nasrallah, M.N., Seruggia, D., Usmani, S.M., Misale, S., Zappulli, V., Carrizosa, E., et al. (2019). Targeting the CBM complex causes Treg cells to prime tumours for immune checkpoint therapy. Nature *570*, 112–116.

Fontan, L., Yang, C., Kabaleeswaran, V., Volpon, L., Osborne, M.J., Beltran, E., Garcia, M., Cerchietti, L., Shaknovich, R., Yang, S.N., et al. (2012). MALT1 small molecule inhibitors specifically suppress ABC-DLBCL in vitro and in vivo. Cancer Cell *22*, 812–824.

Fontenot, J.D., Dooley, J.L., Farr, A.G., and Rudensky, A.Y. (2005). Developmental regulation of Foxp3 expression during ontogeny. J. Exp. Med. *202*, 901–906.

Friedman, C.F., Proverbs-Singh, T.A., and Postow, M.A. (2016). Treatment of the immune-related adverse effects of immune checkpoint inhibitors: a review. JAMA Oncol. *2*, 1346–1353.

Gewies, A., Gorka, O., Bergmann, H., Pechloff, K., Petermann, F., Jeltsch, K.M., Rudelius, M., Kriegsmann, M., Weichert, W., Horsch, M., et al. (2014). Uncoupling Malt1 threshold function from paracaspase activity results in destructive autoimmune inflammation. Cell Rep. *9*, 1292–1305.

Hameyer, D., Loonstra, A., Eshkind, L., Schmitt, S., Antunes, C., Groen, A., Bindels, E., Jonkers, J., Krimpenfort, P., Meuwissen, R., et al. (2007). Toxicity of ligand-dependent Cre recombinases and generation of a conditional Cre deleter mouse allowing mosaic recombination in peripheral tissues. Physiol. Genomics *31*, 32–41.

Jacobs, K.A., Andre-Gregoire, G., Maghe, C., Thys, A., Li, Y., Harford-Wright, E., Trillet, K., Douanne, T., Alves Nicolau, C., Frenel, J.S., et al. (2020). Paracaspase MALT1 regulates glioma cell survival by controlling endo-lysosome homeostasis. EMBO J. *39*, e102030.

Jaworski, M., Marsland, B.J., Gehrig, J., Held, W., Favre, S., Luther, S.A., Perroud, M., Golshayan, D., Gaide, O., and Thome, M. (2014). Malt1 protease inactivation efficiently dampens immune responses but causes spontaneous autoimmunity. EMBO J. *33*, 2765–2781.

Jeltsch, K.M., Hu, D., Brenner, S., Zoller, J., Heinz, G.A., Nagel, D., Vogel, K.U., Rehage, N., Warth, S.C., Edelmann, S.L., et al. (2014). Cleavage of roquin and regnase-1 by the paracaspase MALT1 releases their cooperatively repressed targets to promote T(H)17 differentiation. Nat. Immunol. *15*, 1079–1089.

Johncilla, M., Grover, S., Zhang, X., Jain, D., and Srivastava, A. (2019). Morphological spectrum of immune checkpoint inhibitor therapy associated gastritis. Histopathology *76*, 531–539.

Juilland, M., and Thome, M. (2016). Role of the CARMA1/BCL10/MALT1 complex in lymphoid malignancies. Curr. Opin. Hematol. *23*, 402–409.

Lork, M., Staal, J., and Beyaert, R. (2019). Ubiquitination and phosphorylation of the CARD11-BCL10-MALT1 signalosome in T cells. Cell Immunol. *340*, 103877.

Luche, H., Weber, O., Nageswara Rao, T., Blum, C., and Fehling, H.J. (2007). Faithful activation of an extra-bright red fluorescent protein in "knock-in" Cre-reporter mice ideally suited for lineage tracing studies. Eur. J. Immunol. *37*, 43–53.

Martin, K., Junker, U., Tritto, E., Sutter, E., Rubic-Schneider, T., Morgan, H., Niwa, S., Li, J., Schlapbach, A., Walker, D., et al. (2020a). Pharmacological inhibition of MALT1 protease leads to a progressive IPEX-like pathology. Front. Immunol. *11*, 745.

Martin, K., Touil, R., Cvijetic, G., Israel, L., Kolb, Y., Sarret, S., Valeaux, S., Degl'innocenti, E., Le Meur, T., Nadja, C., et al. (2020b). MALT1 protease activity is required for FcgammaR-induced arthritis but not FcgammaR-mediated platelet elimination in mice. Arthritis Rheumatol. *72*, 919–930.

Martin, K., Touil, R., Kolb, Y., Cvijetic, G., Murakami, K., Israel, L., Duraes, F., Buffet, D., Gluck, A., Niwa, S., et al. (2019). Malt1 protease deficiency in mice disrupts immune homeostasis at environmental barriers and drives systemic T cell-mediated autoimmunity. J. Immunol. *203*, 2791–2806.

Mc Guire, C., Elton, L., Wieghofer, P., Staal, J., Voet, S., Demeyer, A., Nagel, D., Krappmann, D., Prinz, M., Beyaert, R., et al. (2014). Pharmacological inhibition of MALT1 protease activity protects mice in a mouse model of multiple sclerosis. J. Neuroinflammation *11*, 124.

Nagel, D., Spranger, S., Vincendeau, M., Grau, M., Raffegerst, S., Kloo, B., Hlahla, D., Neuenschwander, M., Peter Von Kries, J., Hadian, K., et al. (2012). Pharmacologic inhibition of MALT1 protease by phenothiazines as a therapeutic approach for the treatment of aggressive ABC-DLBCL. Cancer Cell *22*, 825–837.

Oeckinghaus, A., Wegener, E., Welteke, V., Ferch, U., Arslan, S.C., Ruland, J., Scheidereit, C., and Krappmann, D. (2007). Malt1 ubiquitination triggers NF-kappaB signaling upon T-cell activation. EMBO J. *26*, 4634–4645.

Pipi, E., Nayar, S., Gardner, D.H., Colafrancesco, S., Smith, C., and Barone, F. (2018). Tertiary lymphoid structures: autoimmunity goes local. Front. Immunol. *9*, 1952.

Rosenbaum, M., Gewies, A., Pechloff, K., Heuser, C., Engleitner, T., Gehring, T., Hartjes, L., Krebs, S., Krappmann, D., Kriegsmann, M., et al. (2019). Bcl10-controlled Malt1 paracaspase activity is key for the immune suppressive function of regulatory T cells. Nat. Commun. *10*, 2352.

Ruland, J., and Hartjes, L. (2019). CARD-BCL-10-MALT1 signalling in protective and pathological immunity. Nat. Rev. Immunol. *19*, 118–134.

Staal, J., Driege, Y., Bekaert, T., Demeyer, A., Muyllaert, D., Van Damme, P., Gevaert, K., and Beyaert, R. (2011). T-cell receptor-induced JNK activation requires proteolytic inactivation of CYLD by MALT1. EMBO J. *30*, 1742–1752.

Sun, L., Deng, L., Ea, C.K., Xia, Z.P., and Chen, Z.J. (2004). The TRAF6 ubiquitin ligase and TAK1 kinase mediate IKK activation by BCL10 and MALT1 in T lymphocytes. Mol. Cell *14*, 289–301.

Uehata, T., Iwasaki, H., Vandenbon, A., Matsushita, K., Hernandez-Cuellar, E., Kuniyoshi, K., Satoh, T., Mino, T., Suzuki, Y., Standley, D.M., et al. (2013). Malt1-induced cleavage of regnase-1 in CD4(+) helper T cells regulates immune activation. Cell *153*, 1036–1049.

Verespy, S., 3rd, Mehta, A.Y., Afosah, D., Al-Horani, R.A., and Desai, U.R. (2016). Allosteric partial inhibition of monomeric proteases. Sulfated coumarins induce regulation, not just inhibition, of thrombin. Sci. Rep. *6*, 24043.

Woodland, D.L., and Randall, T.D. (2004). Anatomical features of anti-viral immunity in the respiratory tract. Semin. Immunol. *16*, 163–170.

Yu, J.W., Hoffman, S., Beal, A.M., Dykon, A., Ringenberg, M.A., Hughes, A.C., Dare, L., Anderson, A.D., Finger, J., Kasparcova, V., et al. (2015). MALT1 protease activity is required for innate and adaptive immune responses. PLoS One *10*, e0127083.

iScience, Volume *23*

Supplemental Information

Long-Term MALT1 Inhibition in Adult Mice Without Severe Systemic Autoimmunity

Annelies Demeyer, Yasmine Driege, Ioannis Skordos, Julie Coudenys, Kelly Lemeire, Dirk Elewaut, Jens Staal, and Rudi Beyaert

Supplemental Information

Transparent Methods

Mice

Malt1$^{-/-}$, *Malt1*$^{FL/FL}$ and *Malt1*$^{PD/PD}$ C57Bl/6 mice have been described previously (Demeyer et al., 2019). *Malt1*-i-PD mice and control mice were respectively *Malt1*$^{PD/FL}$ and *Malt1*$^{+/FL}$ C57Bl/6 mice with a tamoxifen-inducible Cre-ERT2 transgene in one *Rosa26* allele (Hameyer et al., 2007), and a LoxP-stop-LoxP (LSL) RFP reporter gene in the other *Rosa26* allele (Luche et al., 2007). All mice were maintained under specific-pathogen free conditions and fed *ad libitum* at the animal house of the VIB/UGent Center for Inflammation Research. Experiments were carried out in accordance with the UGent ethical guidelines and approved by the local ethical committee for mouse experiments of the VIB-Ghent University Faculty of Sciences (approval numbers EC 2015-031, EC2019-081 and EC2019-082). Equal results were obtained with male and female mice unless otherwise specified.

Single cell suspensions and stimulation

Spleens and thymi were mechanically disrupted with the plunger of a syringe and filtered over a 70 µm cell strainer. For the isolation and analysis of DCs, splenocytes were cut in small pieces and incubated at 37°C for 30 minutes in RPMI 1640 containing Liberase TM (Roche, Mannheim, Germany) and DNase I (Roche). All single cell suspensions were subjected to red blood cell lysis with ACK lysis buffer (Lonza).

To assess intracellular cytokine production, spleen single cell suspensions were cultured in complete medium (RPMI 1640 medium supplemented with 10% FCS, sodium pyruvate, L-glutamine, antibiotics and β-mercaptoethanol) and stimulated with PMA (50ng/ml), ionomycin (500ng/ml) and brefeldin A (1µg/ml) for 4 hours at 37°C and 5% CO2.

To assess MALT1 protease activity, spleen single cell suspensions were cultured in complete medium and left unstimulated or stimulated with PMA (200ng/ml) and ionomycin (1µM) for 90 min at 37°C and 5% CO2.

Immunoblot analysis

Splenocytes were lysed in 50 mM Hepes pH 7.6, 250 mM NaCl, 5 mM EDTA, and 0.5% (vol/vol) NP-40, plus phosphatase and protease inhibitors. Lysates were cleared by centrifugation for 15 min at 14,000 rpm and

4°C. Protein concentration was measured by Bradford protein assay (Bio-Rad) and 5x Laemmli buffer (250 mM Tris-HCl pH 8, 10% SDS, 50% glycerol, 0.005% bromophenol blue, 25% β-mercaptoethanol) was added to the lysates. Equal amounts of protein were separated by 8% or 10% SDS–PAGE and analyzed by semi-dry immunoblotting and detection via enhanced chemiluminescence (Perkin-Elmer Life Sciences). The antibodies that were used are anti-BCL10 cleavage-specific (gift from Thijs Baens, Cistim Leuven vzw, Leuven, Belgium), anti-CYLD (sc-74435, Santa Cruz), anti-HOIL1 (sc365523, Santa Cruz), anti-β-actin-HRP (sc-47778, Santa Cruz), HRP-conjugated anti-mouse and anti-rabbit IgG antibody (Thermo Fisher Scientific 31432 and 31464).

Flow cytometry

Splenocytes, thymocytes and blood cells were analyzed with a LSRII or a Fortessa 5 flow cytometer (BD Biosciences) and FlowJo Software (Treestar, Inc, Ashland, Ore) was used for data analysis. Cells were stained for 20 min at 4°C with master mix containing a fixable live/dead dye eFluor 506 or eFluor780, FC block anti-CD16/CD32 and antibodies against surface antigens. Cells were analyzed unfixed or fixed for 30 min at 4°C with the BD Cytofix/cytoperm Kit or the eBioscience Foxp3/Transcription Factor staining buffer set. After fixing, intracellular antigens were stained by adding the corresponding antibodies in the permeabilization solution from the corresponding fixative buffer set for 30 min at 4°C. Antibodies were purchased from BD Biosciences, eBioscience, Thermo Fisher Scientific or Tonbo Bioscience. The following antibodies were used CD3 (145-2C11 or 17A2), CD4 (RM4-5 or GK1.5), CD8 (53-6.7), CD25 (PC61), CD44 (IM7), CD62L (MEL-14), CD11b (M1/70), CD11c (N418), FoxP3 (FJL-16s), TNFR2 (TR75-89), CTLA4 (UC10-4B9), IL-2 (JES6-5H4), IFN-γ (XMG1.2), TNF (MP6-XT22), CD19 (1D3), CD45R/B220 (RA3-6B2), CD21/CD35 (4E3), CD23 (B3B4), Siglec H (440c), Ly6-C (AL-21), NKp46 (29A1.4), Ly6-G (1A8), MHCII (M5/114.15.2), CD172a (P84).

Histology

Stomach, lungs, salivary glands, colon and liver were fixed with 4% paraformaldehyde and imbedded in paraffin. Sections (5 µm) were stained with haematoxylin and eosin. Scoring of immune cell infiltration in lungs and stomach was done blinded. Lung and stomach sections were stained with anti-CD3 (A0452, Dako-Agilent Technologies) or anti-B220 (RA3-6B2, eBioscience) and counterstained with haematoxylin. Images (100x magnification) were acquired with a BX51 discussion microscope (Olympus) using an objective lens with

N.A. 1.0. The 100 µm scale bar was added with Fiji.

Cytokine detection in blood

Blood samples were collected for serum preparation and the levels of IL-5 (171-G5006M), IL-10 (171-G5009M), IL-13 (171-G5012M), IL-17 (171-G5013M), KC (171-G5018M), IFN-γ (171-G5017M) and TNF (171-G5023M) were determined by Bio-Plex (Biorad) according to the manufacturer's conditions.

Statistics

GraphPad Prism 8 software was used for all statistical analysis. Data are represented as means ± SEM. P values were calculated by unpaired Student's t-test, and differences between groups were considered statistically significant with a P value lower than 0.05 or less; *$p < 0.05$, **$p < 0.01$, ***$p < 0.001$, and ****$p < 0.0001$.

Figure S1. *Malt1*-i-PD mice have no autoantibodies in their serum after 6 months tamoxifen, Related to Figure 4. Picture of line immunoassay strips (INNO-LIA ANA Update, Fujirebio) to detect specific antibodies from *Malt1*-i-PD mice. Serum of healthy C57BL/6 mice and serum from a NOD mouse were included as negative and positive controls, respectively. Each strip corresponds to an individual mouse. The assay contains the following recombinant and natural antigens: SmB, SmD, RNP-A, RNP-C, RNP-70k, Ro52/SSA, Ro60/SSA, La/SSB, CenpB, Topo-I/Scl70, Jo-1, ribosomal P, and histones. Nylon strips were incubated with mouse serum at a 1:200 dilution. Following washing, a 1:2,500 dilution of alkaline phosphatase-conjugated anti-mouse IgG was added (Chemicon). After washing, addition of the chromogen 5-bromo-4-chloro-3-indolyl phosphate produced a dark brown color in proportion to the amount of specific autoantibody in the test sample. Sulfuric acid was added to stop the color development.